Engineered Science

RESEARCH PAPER View Article Online

# PbS Sensitized $TiO_2$ Based Quantum Dot Solar Cells with Efficiency Greater Than 5 % Under Artificial Light: Effect of Compact Layer and Surface Passivation

Vikram P. Bhalekar, Prashant K. Baviskar*, Rajendra Prasad M. B., Balasaheb M. Palve, Vishal S. Kadam and Habib M. Pathan*

Now days, quantum dot sensitized solar cells have fascinated a great deal of interest due to its advantages that include high molar extinction coefficient, tunable energy gaps, and multiple exciton generation of quantum dots. In this present work, the linker free approach was used to sensitize $TiO_2$ photoelectrodes with PbS QDs by successive ionic layer adsorption and reaction at room temperature. The photovoltaic performance was evaluated using J-V characteristics with polysulphide as electrolyte and carbon composite molybdenum oxide as a counter electrode using Keithley Source meter under white light (30 mW/cm$^2$) supplied from LED source. Electrochemical impedance spectroscopy is also used to measure the electron life time of the devices using Potentiostat/Galvanostat. Maximum efficiency of 5.82 % was recorded under artificial light with addition of $TiO_2$ compact layer prior to porous $TiO_2$ followed by surface passivation of PbS using ZnS, which corresponds to ~3 fold enhancement to that of device fabricated using bare $TiO_2$.

**Keywords**: $TiO_2$; PbS; Quantum dot sensitized solar cells; Effect of compact layer; Surface passivation

**Received** 5 October 2018, **Accepted** 17 January 2019

**DOI:** 10.30919/es8d676

## Introduction

Quantum dots (QDs) define the scope for the modern world that opens up the new trends in both fundamentals and commercial point of view hence it is being excited to study. Quantum dot solar cells are emerging out as an alternative strategy towards replacement of expensive dye with semiconductor QDs as sensitizers due to its photostability, high molar extinction coefficient, size dependent optical properties and low cost.[1] The electronic affinity and optical band gap of QDs can be tuned by altering the particle size without changing the chemical composition.[2] The various reports are available on quantum dots sensitized solar cells (QDSSCs) sensitized with PbS,[3] CdS,[4,5] CdSe,[6] CdTe,[7] $Ag_2Se$,[8] $Bi_2S_3$,[9] etc. Recently, researchers have a discovery about multiple exciton generation (MEG).[10,11] Out of that, lead sulphide (PbS) becomes favorable candidate because of their large Bohr exciton radius of 20 nm.[12,13] PbS is IV-VI direct band gap semiconductor with bulk band gap 0.41 eV,[14] which is tuned to 1.3 eV and allows the panchromatic utilization of the solar spectrum extends to near infra-red region. Hence it becomes an interesting and easy costumer for solar cell applications.[15] Lee *et al*. reported the PCE of 5.6 % for Hg doped PbS sensitized $TiO_2$ based QDSSC using SILAR technique.[16] The maximum efficiency of 5.73 % was reported by Sung *et al*. for PbS QDs sensitized bilayered $TiO_2$ nanostructure as a photoanode with aq. polysulfide electrolyte and Au/CuS/FTO as counter electrode.[15] It is also reported that by introducing a compact $TiO_2$ as a blocking layer prior to porous metal oxide can efficiently prevent the backward transfer of electrons and help towards the enhancement in efficiency.[17,18]The alternate strategy to improve the photovoltaic performance of QDSSC is the surface modification of QDs which is beneficial towards the reduction in charge recombination at internal QDs as well as at QDs/metal oxide/electrolyte interfaces and avoid corrosion due to the polysulfide electrolyte.[19,20] In addition to compact and surface passivation layers, the development of new counter electrodes (CEs) with high electrocatalytic activity, good conductivity, and stability are crucial for performance enhancement of QDSSCs. Therefore, in recent time much attention has been focused on developing a range of CEs for QDSSCs alternative to Pt.[21-24]

We have focused on chemical sensitization of PbS QDs over porous $TiO_2$ prepared by doctor blade technique on compact $TiO_2$/FTO substrate towards fabrication of solar cell. Here we have used SILAR technique for the sensitization of PbS over $TiO_2$ photoelectrode followed by surface passivation of PbS using ZnS layer by SILAR towards the performance enhancement of solar cell.

## Experimental section

### Materials used

$TiO_2$ powders (P25) was purchased from Degussa, Ethyl cellulose, Terpanol, Acetyl acetone, Lead nitrate, Sodium sulphide, and Sulphur powder were purchased from SRL Chemicals Ltd., whereas Ethanol and Methanol were purchased from C.H. Fine Chemicals Co. Ltd. and were used as received without any further purification. Fluorine doped tin oxide (FTO) (sheet resistance of ~12 Ω/cm$^2$ from Sigma Aldrich, India) coated conducting glass substrates were cut into a size of 2 x 2 cm$^2$. These were initially cleaned by using double distilled water then with a soap solution followed by ultrasonication for 15 min in double distilled water and ethanol and finally, the films were allowed to dry in incubator at 70°C till use.

### Deposition of $TiO_2$ compact layer

Initially, prepare the solution by taking 5 ml $TiCl_3$ in 20 ml double distilled water (hereafter, DDW). Then prepare the 1 M NaOH in DDW

*Advanced Physics Laboratory, Department of Physics, Savitribai Phule Pune University, Pune–411007, India*
***E-mail:** pkbaviskar@physics.unipue.ac.in; habib.pathan@gmail.com*

and add it drop wise in $TiCl_3$ solution with constant stirring till it becomes transparent (approx. 7.5 ml). Finally, immersed the pre cleaned FTO substrates in the solution and placed the reaction bath in an incubator maintained at 45°C for 15 hr. The film shows a compact layer which were washed by DDW to remove unbounded excess $TiO_2$ deposition, dried in incubator at 60°C for 1 hr followed by annealing at 450°C for 1 hr. The films are then ready for the further deposition of porous $TiO_2$ layer.

### Preparation of porous $TiO_2$ films

Initially; the paste was prepared using P25 degussa $TiO_2$ powder by grinding in ethanol, ethyl cellulose; terpanol through ultrasonication for 4 hr., then by adding acetyl acetone. Finally, a white paste (slurry) is ready to make the $TiO_2$ films.

Was used to deposit $TiO_2$ films using prepared paste on bare FTO and compact $TiO_2$/FTO substrates. One may apply layer by layer deposition of $TiO_2$ in order to get appropriate thickness. The thickness of the photoelectrode was optimized for the proper functioning of solar cell (15-20 μm). The films were allowed to dry in oven at 60°C for 15 min after each layer deposition. This procedure was repeated for 8 layer of $TiO_2$ followed by the step heating at 100°C, 200°C and 300°C for 15 min each and then finally at 450°C for 1 hr, so as to remove the organic solvents used during the preparation of paste. The furnace is then allowed to cool so that white transparent films were obtained and used for sensitization, characterization and device fabrication.

### $TiO_2$ sensitization with PbS

$TiO_2$ films with and without compact layer were sensitized using PbS QDs by SILAR technique. For sensitization of $TiO_2$ electrodes; 0.02 M solutions of $Pb(NO_3)_2$ and $Na_2S$ were prepared separately in aqueous and ethanol, respectively. The annealed $TiO_2$ films were then allowed to a have 6 SILAR cycles of PbS over it. Out of 6 SILAR cycles; initial 2 cycles were of 15 sec and the later 4 cycles were of 1 min in each precursor. The colour of the films turned out from white to faint yellow in the beginning after 2 cycles. Afterward the colour of the films was then changed from faint yellow to faint brown and finally to dark brown. As the SILAR cycles were increases the films show colour variation that indicates the growth of PbS QDs on $TiO_2$ surface. After the last cycle the films were again dipped into a lead precursor, such that an additional positive ion plays a role in electron transportation.

### Surface passivation by ZnS

The PbS sensitized porous $TiO_2$ film with compact layer were then allowed to have surface passivation though a loading of ZnS layer over PbS[25] for 2 SILAR cycles.

### Device preparation

The $MoO_3$ coated FTO substrate was used as counter electrode prepares by spray pyrolysis similarly as reported earlier.[26] The assembly was held together using binder clips. The freshly prepared liquid electrolyte solution was injected between PbS sensitized $TiO_2$ photoanode and counter electrode. Sodium sulphide and sulphur powder were taken and grinded separately in ethanol, then by mixing them properly with the addition of 2 ml distilled water and ethanol gives a polysulphide electrolyte ready to use for performance measurement.

#### Instrumentations

The structural studies was carried out using X-ray diffractometry (XRD) (model: XRD, Rigaku "D/B max-2400", $CuK_\alpha$ with λ=1.54 Å) in 2 range of 20-60 degrees. The optical absorption spectra are acquired with JASCO V-670 in the wavelength range of 300 to 1500 nm. The morphology, elementary composition, shape and size of PbS quantum dots was studied by using Scanning electron microscope (SEM) [JEOL-JSM 6360-A operating at 20 kV], Energy dispersive X-ray (EDS) unit coupled with SEM and Transmission Electron Microscope (TEM) (Tecnai $G^2$ 20 Twin, FEI). The photovoltaic characteristics (J-V) were measure using a Keithley source meter (Model: 2420) under white light illumination at 30 mW/$cm^2$ intensity supplied from LED with 0.1 $cm^2$ active illumination area for all the cells. The electrochemical impedance spectroscopy (EIS) study for devices were carried out using potentiostat/galvanostat (IVIUM:Vertex) in the mid and low frequency domain from $10^3$-$10^{-1}$ Hz under dark.

## Results and discussion

Fig. 1(a) shows the XRD pattern of pristine $TiO_2$ and PbS sensitized $TiO_2$ films with and without surface passivatation using ZnS. The XRD patterns of $TiO_2$ showed peaks at 2θ = 25.5°, 37.8°, 48.2°, 53.9°, and 62.5°, which were indexed to tetragonal structure $TiO_2$ of anatase phase (JCPDS: 21-1272) and the additional peak at 2θ = 27.6° is observed correspond to (110) plan of rutile $TiO_2$ (JCPDS: 21-1272). For PbS sensitized $TiO_2$ the additional peaks are observed at 2θ = 30.1° and 43.1° which are corresponding to the (200) and (220) planes of cubic PbS (JCPDS: 78-1058). Similarly, the peaks at 2θ = 36.2° for ZnS passivated PbS sensitized $TiO_2$ film is indexed to (105) crystal plane of the hexagonal ZnS (JCPDS: 89-2739). After the ZnS coating, the increase in peak broadening at around 30° also indicates that the PbS QDs are covered with ZnS.[27] The XRD results validate the sensitization of PbS over $TiO_2$ surface and surface passivation of PbS with ZnS. The peaks of $TiO_2$, PbS and ZnS were highlighted by notation T, P and Z, respectively.

For a both $TiO_2$ films loaded with PbS QDs is as shown in Fig. 1(b). It shows the absorbance peak for $TiO_2$ at 374 nm and that for PbS is at 848 nm over $TiO_2$. The longest absorption wavelength ($\lambda_{onset}$) was used to calculate the optical energy gap ($E_g$) according to the equation[28] and found to be 1.46 eV for PbS. It is observed that with loading of PbS; the absorbance region extended/ shifted towards the higher wavelength. In order to maintain the proper thickness of $TiO_2$, all the experimental conditions are identical like concentration, temperature, time for deposition etc. Because as the particle size increases it blocks the pores of $TiO_2$ and so the PbS cannot go inside to fill the pores as it covers the total surface and hence number of adsorbed ions decreases. This leads to lower the performance of the solar cells. To suppress charge recombination, the surface passivation of PbS using ZnS were performed as mentioned earlier.[29] According to Braga *et al.*[30] the conduction band of bulk PbS is lower than $TiO_2$ but as the size of PbS decreases below 18 nm its position shifted above $TiO_2$ and hence there is path for electron transportation. Fig. 1(c) shows the top view of PbS sensitized $TiO_2$ film was examined using SEM to analyze the surface morphology. It was observed that the sample were granular structure and porous in nature. It is clearly observed that the coating of PbS QDs over the entire surface as well as in between the pours of $TiO_2$ film. On top, agglomeration of tiny particles leads to the formation of the bigger particles of PbS. Inset (c) shows the presence of Ti, O along with Pb and S in sample confirm the sensitization of $TiO_2$ with PbS). From Fig. 1(d) TEM and histogram analysis (inset) it is observed that the size of the PbS prepared by SILAR in the present study is in the range of 4-8 nm.

Shows the representation of bottom-up approach towards the development of efficient device with addition of compact layer followed by surface passivation of PbS QDs using ZnS. The deposition of $TiO_2$

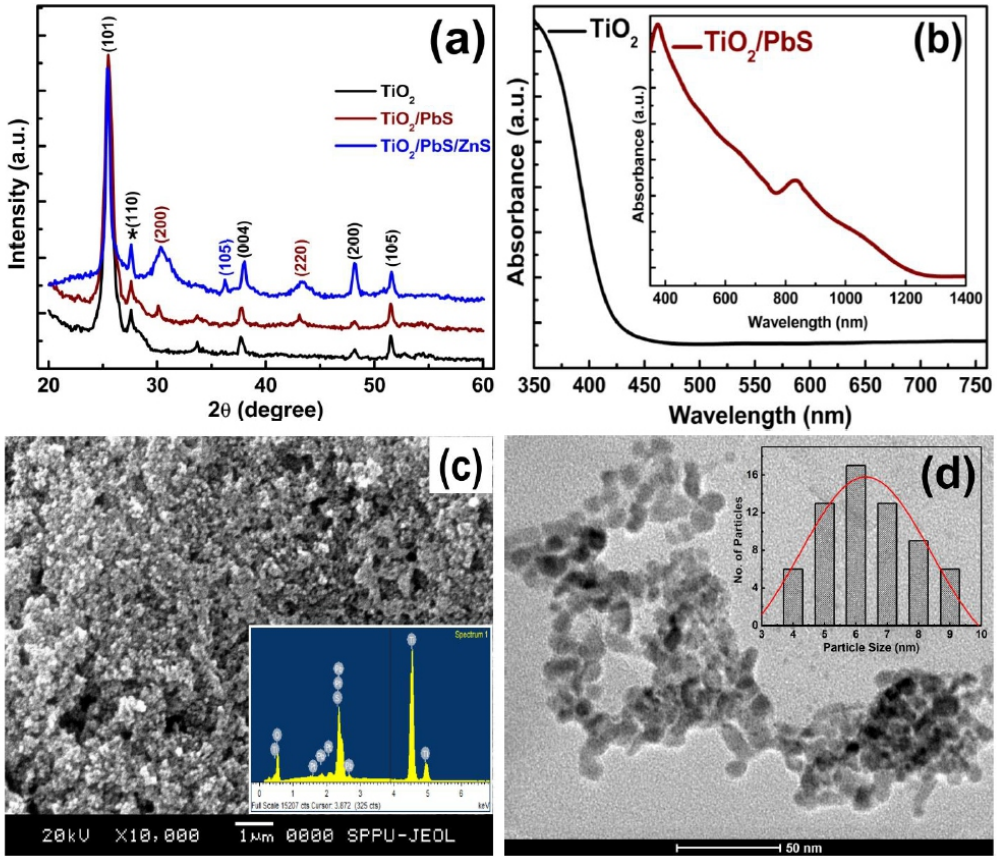


**Fig. 1** (a) XRD plots of pristine $TiO_2$, PbS sensitized $TiO_2$ and surface passivated PbS sensitized $TiO_2$ films. (b) Optical absorption spectra for pristine $TiO_2$ and PbS sensitized $TiO_2$ films. (c) SEM image of PbS sensitized $TiO_2$ and inset shows the EDS spectra of the same sample. (d) TEM image of PbS QDs and inset show size distribution of PbS QDs (Histogram).

blocking layer on the FTO surface prior to the deposition of porous $TiO_2$ layer play a vital role towards the enhancement in photocurrent as it avoid the direct contact of the FTO surface with the redox electrolyte. ZnS as surface passivation layer over PbS is coated to suppress back electron transfer to the electrolyte. The polysulfide electrolyte is acts as a hole transporter material and $MoO_3$-based counter electrode. Schematic device structure with energy band diagram for FTO/$TiO_2$/PbS/ZnS/Electrolyte/Counter is shown in Fig. 2(b).[31,32] Under illumination of light, the PbS QDs on the photoanodes harvest some light within a certain region of wavelengths according to their band gap to generate photo-excited electrons, which are subsequently injected from the conduction band (CB) of the PbS QDs into the CB of the $TiO_2$ semiconductor and then quickly migrated to the external circuit through the FTO substrate. Meanwhile, holes remain in the valence band (VB) of the PbS QDs, which are immediately transferred to the redox electrolyte to oxidize it. The oxidized electrolyte is restored by the electrons supplied through the $MoO_3$ CE from the external circuit back to the cycling circuit in the cell.[33] There is possibility of interfacial recombination of electrons from PbS and the $TiO_2$ with the oxidized form electrolyte. This interfacial recombination of electrons can be suppressed by use of ZnS surface passivation layer over PbS sensitized $TiO_2$.

Density-voltage (J-V) characteristics of all the three devices is depict as Fig. 2(c). The performance factor includes open circuit voltage ($V_{oc}$), short-circuit current ($J_{sc}$), fill factor (FF) and power conversion efficiency (PCE). The performance comparison is summarized in Table 1. From table it is observed that the $TiO_2$ photoanode made using P25 degussa powder with compact layer and surface passivation of PbS QDs using ZnS shows a higher performance as compared to photoanode made using bare $TiO_2$ and $TiO_2$ with only compact layer.

Electrochemical impedance spectroscopy (EIS) under dark for all the three $TiO_2$ photoanodes sensitized with PbS QDs was recorded under open circuit (V = 0.55V). In present study, two semicircles are observed in the Nyquist plot, the first semicircle in high frequency range denotes the charge transfer resistance (RCE) at interface of CE/ electrolyte, while large and second semicircle in mid frequency suggesting the charge transfer resistance ($R_{ct}$) at the $TiO_2$/QDs/electrolyte interfaces. The series resistance of transparent conducting oxide is represented by Rs, which is evaluated at the high frequency region. The series resistance ($R_s$) is the nonzero intercept on the real axis of the impedance plot, which denotes the sheet resistance of TCO and the contact resistance of FTO/$TiO_2$.[34,35] From Nyquist plot (Fig. 2(d)), it is observed that the radius of second semicircle increases after addition of compact $TiO_2$ layer. The addition of compact layer will efficiently prevent the direct contact between FTO and counter electrode as well as help towards the enhancement in efficiency of solar cell. Furthermore, the surface passivation of PbS QDs using ZnS layer considerably enhanced the overall performance of device by preventing the interfacial recombination. The intermediate frequency gives recombination resistance ($TiO_2$/PbS QDs/electrolyte interface) as per earlier results.[3] The relatively lower fill factor of observed for all the devices is mainly due to the higher series resistance ($R_s$) observed from Nyquist plot.[36]

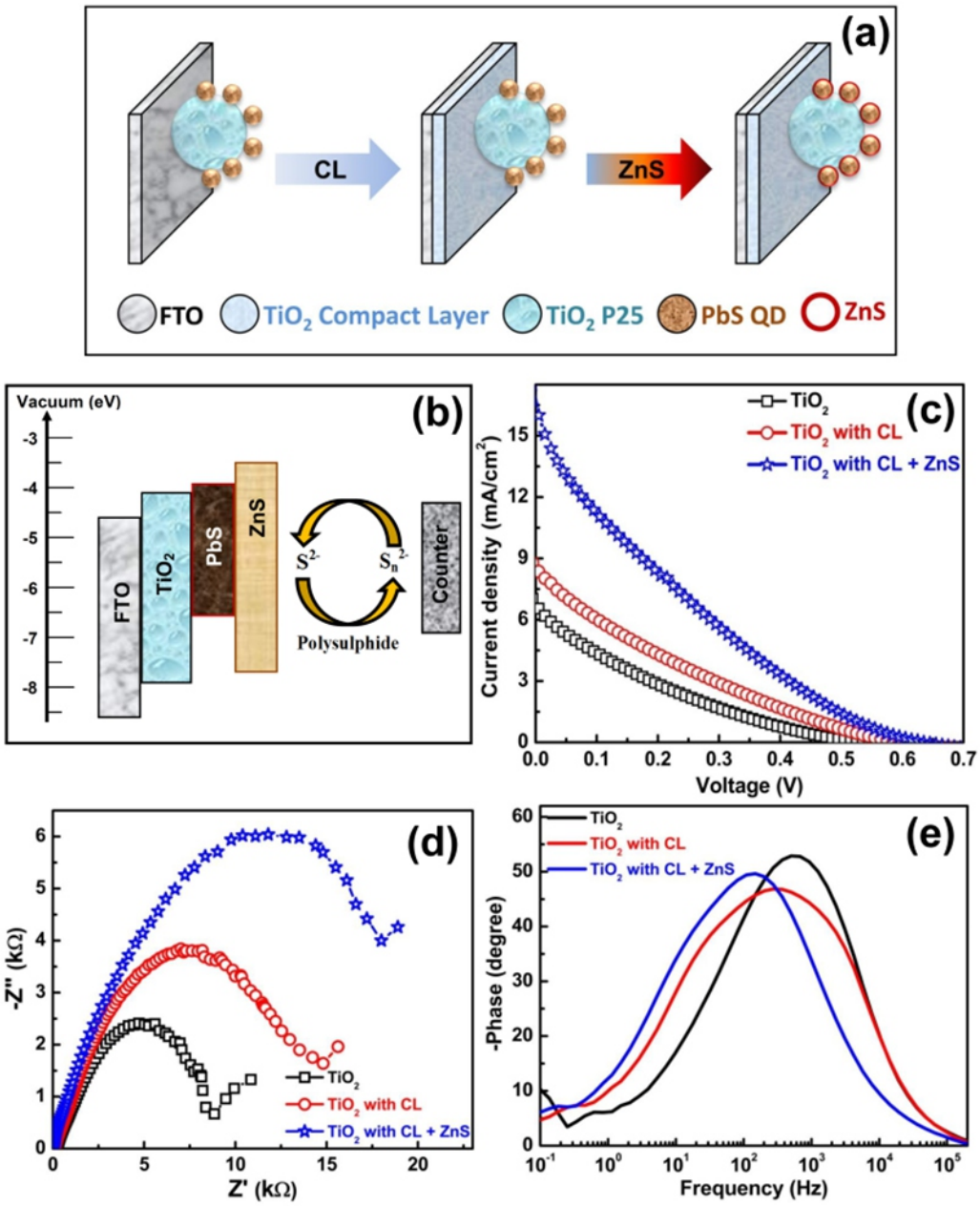


**Fig. 2** (a) Schematic showing the bottom-up approach towards the development of architecture for efficient solar cell. (b) Energy band diagram[25,26], (c) Current density-voltage (J-V) curves, (d) Nyquist plot and (e) Bode plot for ZnS passivated PbS QDs sensitized $TiO_2$ solar cells with $MoO_3$ as counter electrode.

**Table 1** The performance comparison for PbS sensitized $TiO_2$ photoanode quantum dot solar cells.

| $TiO_2$ with | $V_{oc}$ (V) | $J_{sc}$ (mA/cm$^2$) | FF (%) | $\tau_e$ (ms) | $R_s$ (Ω) | $R_{ct}$ (kΩ) | PCE (%) |
|---|---|---|---|---|---|---|---|
| - | 0.52 | 6.78 | 16 | 0.31 | 240 | 8.32 | 1.90 |
| CL | 0.59 | 8.57 | 17 | 0.58 | 114 | 14.69 | 2.98 |
| CL + ZnS‡ | 0.63 | 16.74 | 16 | 1.07 | 35 | 17.96 | 5.82 |

‡CL: Compact Layer; ZnS: Surface Passivation Layer

Bode plots as shown in Fig. 2(e) gives the electron life time according to the equation $\tau_e = 1/(2\pi f)$.[37] The value of charge recombination resistance ($R_{ct}$) measured from Nyquist plot using second semicircle in mid frequency region and electron life time ($\tau_e$) calculated from Bode plot were summarized in table 1 for all three devices.

## Conclusions

This research work demonstrate that the effect of addition of compact layer prior to porous $TiO_2$ and surface passivation treatment over PbS QDs. PbS QDs are directly loaded on $TiO_2$ photoelectrodes by SILAR technique at room temperature in reproducible and controllable manner for QDSSC application. It is observed that the performance of QDSSC improves with the addition of compact $TiO_2$ layer prior to the porous $TiO_2$. The maximum efficient of 5.82 % was recorded for $TiO_2$ photoanode with compact layer and using surface passivation of PbS by ZnS with polysulphide electrolyte and molybdenum oxide as a counter electrode. From EIS analysis it is also observed that the charge recombination resistance and electron lifetime for $TiO_2$ photoanode with compact and surface passivation layer based device is considerably higher than other two photoanode based devices. This novel approach accomplished the suppression of recombination losses significantly results into enhancement in device efficiency by ~3 folds and opens a window for further development towards low-cost technology with other metal oxides and chalcogenide QDs.

## Acknowledgements

Authors are thankful to Departmental Research Development Program, SPPU, Pune. PKB is thankful to University Grants Commission, New Delhi, India for the award of Dr. D. S. Kothari Post Doctoral Fellowship and financial assistance (PH/16-17/0074).

## References

1. Z. Yang, C. Y. Chen, P. Roy and H. T. Chang, *Chem. Commun*., 2011, **47,** 9561.
2. L. M. Peter, D. J. Riley, E. J. Tull and K. G. U. Wijayantha, *Chem. Commun*., 2002, **10,** 1030.
3. V. P. Bhalekar, P. K. Baviskar, B. Prasad, N. I. Beedri, V. S. Kadam and H. M. Pathan, *Chem. Phys. Lett*., 2017, **689**, 15.
4. X. Chen, Z. Lan, S. Zhang, J. Wu and J. Zhang, *Optic. Comm,* 2017, **395**, 111.
5. Z. Lan, W. Wu, S. Zhang, L. Que and J. Wu, *Ceram. Int*. 2016, **42**, 8058.
6. H. Zhang, K. Cheng, Y. M. Hou, Z. Fang, Z. X. Pan, W. J. Wu, J. L. Hua and X. H. Zhong, *Chem. Commun*., 2012, **48,** 11235.
7. L. Sai and X. Y. Kong, *Appl. Phys. A*, 2014, **114,** 1153.
8. Q. Tian, D. Deng, Z. Zhang, Y. Li, Y. Yang and X. Guo, *J. Mater. Sci*., 2017, **52,** 12131.
9. P. R. Nikam, P. K. Baviskar, J. V. Sali, K. V. Gurav, J. H. Kim and B. R. Sankapal, *Ceram. Int*., 2015, **41,** 10394.
10. H. Lee, H. C. Leventis, S. J. Moon, P. Chen, S. Ito, S. A. Haque, T. Torres, F. Nuesch, T. Geiger, S. M. Zakeeruddin, M. Gratzel and M. K. Nazeeruddin, *Adv. Funct. Mater.*, 2009, **19,** 2735.
11. I. Robel, V. Subramanian, M. Kuno and P. V. Kamat, *J. Am. Chem. Soc.*, 2006, **128,** 2385.
12. G. D. Scholes and G. Rumbles, *Nat. Mater.*, 2006, **5,** 683.
13. F. W. Wise, Acc. *Chem. Res*., 2000, **33,** 773.
14. V. Gonzalez-Pedro, C. Sima, G. Marzari, P.P. Boix, S. Gimenez, Q. Shen, T. Dittrich and I. Mora-Sero, *Phys. Chem. Chem. Phys.,* 2013, **15,** 13835.
15. S. D. Sung, I. Lim, P. Kang, C. Lee and W. I. Lee, *Chem. Commun.*, 2013, **49,** 6054.
16. J. W. Lee, D. Y. Son, T. K. Ahn, H. W. Shin, I. Y. Kim, S. J. Hwang, M. J. Ko, S. Sul, H. Han and N. G. Park, *Sci. Rep.,* 2013, **3,** 1050.
17. S. Zhang, Z. Lan, J. Wu, X. Chen and C. Zhang, *J. Alloy. Compd.,* 2016, **656,** 253.
18. M. B. R. Prasad, V. Kadam, O. S. Joo and H. M. Pathan, *Mater. Chem. Phys*., 2017, **194**, 165.
19. C. V. V. M. Gopi, M. Venkata-Haritha, Y. S. Lee and H. J. Kim, *J. Mater. Chem. A,* 2016, **4**, 8161.
20. K. Zhao, Z. Pan, I. Mora-Sero, E. Canovas, H. Wang, Y. Song, X. Gong, J. Wang, M. Bonn, J. Bisquert and X. Zhong, *J. Am. Chem. Soc.*, 2015, **137**, 5602.
21. C. V. V. M. Gopi, S. Singh, A. E. Reddy and H. J. Kim, *ACS Appl. Mater. Inter.*, 2018, **10**, 10036.
22. C. V. V. M. Gopi, S. Ravi, S. S. Rao, A.E. Reddy and H. J. Kim, *Sci. Rep.*, 2017, **7**, 46519.
23. C. V. V. M. Gopi, M. Venkata-Haritha, S. K. Kim and H. J. Kim, *J. Power Sources,* 2016, **311**, 111.
24. C.V.V.M. Gopi, M. Venkata-Haritha, S. Ravi, C. V. Thulasi-Varma, S. K. Kim and H. J. Kim, *J. Mater. Chem. C*, 2015, **3**, 12514.
25. S. Hachiya, Q. Shen and T. Toyoda, *J. Appl. Phys.*, 2012, **111**, 104315.
26. P. S. Tamboli, M. B. R. Prasad, V. S. Kadam, R. S. Vhatkar, *Sol. Energy Mater. Sol. Cells*, 2017, **161**, 96.
27. S. Hachiya Q. Shen and T. Toyoda, *J. Appl. Phys*., 2012, **111**, 104315.
28. M. Mohamed, A. H. Eichborn and S. H. Eichborn, *ECS Transactions,* 2010, **25**, 1.
29. F. Deng, X. Mei, X. Wan, R. Fan, Q. Wu, X. Yan, L. Wan, D. Shi and Y. Xiong, *J. Mater. Sci.: Mater. Electron.*, 2015, **26**, 7635.
30. A. Braga, S. Gimenez, I. Concina, A. Vomiero and I. Mora-Sero, *Phys. Chem. Lett.*, 2011, **2,** 454.
31. S. Luo, H. Shen, W. Hu, Z. Yao, J. Li, D. Oron, N. Wang and H. Lin, *RSC Adv.*, 2016, **6,** 21156.
32. R. K. Kokal, M. Deepa, A. Kalluri, S. Singh, I. Macwan, P. K. Patra and J. Gilarde, *Phys. Chem. Chem. Phys.*, 2017, **19,** 26330.
33. C. V. V. M. Gopi, M. Venkata-Haritha, S. K. Kim and H. J. Kim, *Nanoscale,* 2015, **7**, 12552.
34. C. V. V. M. Gopi, M. Venkata-Haritha, S. K. Kim and H. J. Kim, *Dalton Trans*., 2015, **44**, 630.
35. H. J. Kim, G. C. Xu, C.V.V.M. Gopi, H. Seo, M. Venkata-Haritha and M. Shiratani, *J. Electroanal. Chem*., 2017, **788**, 131.
36. K. Zhao, H. Yu, H. Zhang and X. Zhong, *J. Phys. Chem. C*, 2014, **118**, 5683.
37. S. Majumder, P. K. Baviskar and B. R. Sankapal, *Electrochim. Acta*, 2016, **222**, 100.



 